Measuring small compartmental dimensions with low-q angular double-PGSE NMR: The effect of experimental parameters on signal decay

Noam Shemesh [a], Evren Özarslan [b], Peter J. Basser [b], Yoram Cohen [a,*]

[a] School of Chemistry, The Raymond and Beverly Sackler Faculty of Exact Sciences, Tel Aviv University, Ramat Aviv, 69978 Tel Aviv, Israel
[b] Section on Tissue Biophysics and Biomimetics, NICHD, National Institute of Health, Bethesda, MD, USA

ABSTRACT

In confined geometries, the MR signal attenuation obtained from single pulsed gradient spin echo (s-PGSE) experiments reflects the dimension of the compartment, and in some cases, its geometry. However, to measure compartment size, high q-values must be applied, requiring high gradient strengths and/or long pulse durations and diffusion times. The angular double PGSE (d-PGSE) experiment has been proposed as a means to extract dimensions of confined geometries using low q-values. In one realization of the d-PGSE experiment, the first gradient pair is fixed along the x-axis, and the orientation of the second gradient pair is varied in the X–Y plane. Such a measurement is sensitive to microscopic anisotropy induced by the boundaries of the restricting compartment, and allows extraction of the compartment dimension. In this study, we have juxtaposed angular d-PGSE experiments and simulations to extract sizes from well-characterized NMR phantoms consisting of water filled microcapillaries. We are able to accurately extract sizes of small compartments (5 μm) using the angular d-PGSE experiment even when the short gradient pulse (SGP) approximation is violated and over a range of mixing and diffusion times. We conclude that the angular d-PGSE experiment may fill an important niche in characterizing compartment sizes in which restricted diffusion occurs.

© 2009 Elsevier Inc. All rights reserved.

1. Introduction

Diffusion NMR [1] has become important in MR measurements due to its ability to non-invasively measure the mean displacement of molecules [2]. The single pulsed gradient spin echo (s-PGSE) method employs one pair of pulsed magnetic field gradients (PFG) with amplitude and direction given by the vector **G**, which are applied for a duration δ, separated by a diffusion time, $\varDelta$, when spins may diffuse due to Brownian motion. The resulting NMR signal is governed by the phase distribution of molecules produced during the diffusion time, $\varDelta$. The signal attenuation is directly related to the root mean-squared displacement (rmsd) of the diffusing species, which in turn, is directly related to the diffusion coefficient, D, in the case of free diffusion. Since the D is also an indirect measure of the size of molecules, diffusion MR is invaluable for studying supramolecular systems and mixtures of substances [3], degrees of aggregation [4], chemical complexes [5] and even ligand-protein interactions [6].

In isotropic samples, where molecules are free to diffuse in all directions, the logarithm of the NMR signal attenuation is directly related to $b = (\gamma \delta |\mathbf{G}|)^2 t_d$, where γ is the gyromagnetic ratio of the

spins, and t_d is the diffusion time. Especially interesting is when molecules diffuse in a confined geometry, in which case the logarithm of the signal attenuation is no longer linear with respect to b at high b-values [7]. In systems which do not exhibit free diffusion, only an apparent diffusion coefficient (ADC) can be extracted from the plot of the signal decay versus the b values. In recent years it has been shown that the geometry and size of the compartment can be inferred from such s-PGSE experiments, a property which has been utilized in a variety of applications ranging from porous media [8], to biological tissue [9,10]. By measuring the signal decay in several directions, the diffusion tensor can also be estimated [11], providing intrinsic MR parameters that are invariant to rotation. While diffusion tensor imaging (DTI) studies are intended to be performed with low b values ($b < 1500$ s/mm^2), others have conducted diffusion measurements with high b values [9,10,12–16]. In isotropic freely diffusing systems characterized by one compartment, the information that is extracted is the same for both high and low b values, because the natural logarithm of the signal decays linearly when plotted as a function of b. However, in systems characterized by multiple compartments and/or in which different modes of diffusion exist, the attenuation curve deviates from linearity. A diffusion measurement in such systems with high b values can suppress the fast decaying component and accentuate the slow decaying components. Suppressing the fast component often leads

* Corresponding author. Fax: +972 3 6407469.
 E-mail address: ycohen@post.tau.ac.il (Y. Cohen).

to a better estimate of the compartment size [17,18], since the slow component usually arises from spins that remain confined in the restricting compartment whose dephasing is limited.

One of the most important applications of s-PGSE experiments in confined geometries is to extract the size of the compartment. Callaghan et al. showed that in diffusion NMR experiments in regular, ordered confined geometries, a phenomenon called diffusive-diffraction occurs, which is manifested by the non-monotonicity of the signal decay when plotted as a function of $|\boldsymbol{q}|$, where $\boldsymbol{q} = (2\pi)^{-1}\gamma\delta\mathbf{G}$ [19]. The size of the compartment can be extracted from the minima of the signal attenuation curves when plotted as a function of q or from the full-width-at-half-maximum (FWHM) of the probability distribution function (PDF), i.e., from the Fourier Transform (FT) of the signal decay, $E(q)$, as a function of q, provided that the diffusion time is sufficiently long to probe the boundaries of the compartment [20–22]. Exact solutions have been derived for idealized geometries [23–26] and some of these solutions were verified experimentally [22]. Several studies have shown how variation of experimental parameters affects the compartment size that was extracted, including variation of δ, $\varDelta$ and the rotational angle in both phantoms and neuronal tissue [21,22,27,28], however, the need to apply very strong gradients limits the ability to probe the finest spatial dimensions using high $\mathbf{q}$ experiments.

The double-PGSE (d-PGSE) experiment (Fig. 1), which has two pairs of diffusion sensitizing gradients separated by a mixing time (t_{m}), was first proposed by Cory et al. [29] and was applied to studying porous media and flow phenomena [30], 2D diffusion measurements [31,32], suppression of convection artifacts [33], and dispersion and velocity correlation [34,35]. Using the d-PGSE sequence, Callaghan and Komlosh showed microscopic anisotropy in macroscopically isotropic polymers [36]. Recently, Komlosh et al. extended these findings to grey matter and grey matter NMR and MRI phantoms [37,38].

Özarslan and Basser have recently studied the d-PGSE sequence theoretically in the high q regime in confined geometries when the two gradients are parallel [39]. Their findings suggested some unexpected phenomena such as zero-crossings in the NMR signal profile (which result in negative diffractions) that they predicted to be sensitive to prolongation of the mixing time. Shemesh and Cohen have corroborated these findings experimentally, and have shown that, as predicted by simulations in [39], the d-PGSE experiment is sensitive and robust (compared to the s-PGSE) for inferring structural information that can be obtained from complex samples such as mixtures of microcapillaries having different diameters [40].

A limitation of both single and double-PGSE diffraction experiments is that in order to extract the dimension of the restricting compartment, relatively high q values must be reached. Since the q value at which diffractions occur is proportional to the reciprocal of the compartment size, the smaller the compartment, the higher the q that one needs to measure the compartment dimensions. This means that to probe small compartments, which are prevalent, for example, in the central nervous system, there is a need to apply very high q values [23,28], requiring either very strong gradients or very long δs. In such experiments, the finite length of the pulsed gradients makes matters worse, since "motional narrowing" pushes the diffraction minima towards even higher q values, due to a violation of the short gradient pulse (SGP) approximation. To accurately measure the compartment size, δ is assumed to be negligible compared to $\varDelta$. In other words, the SGP approximation assumes that the mean-squared displacement of molecules during the pulsed gradient is insignificant with respect to the mean-squared displacement the molecules will experience during the diffusion period. However, in small compartments, the $\varDelta$ needed for molecules to completely probe the boundaries of the restricting compartment is very short; therefore, δ becomes comparable to $\varDelta$, violating the SGP approximation and resulting in inaccurate size
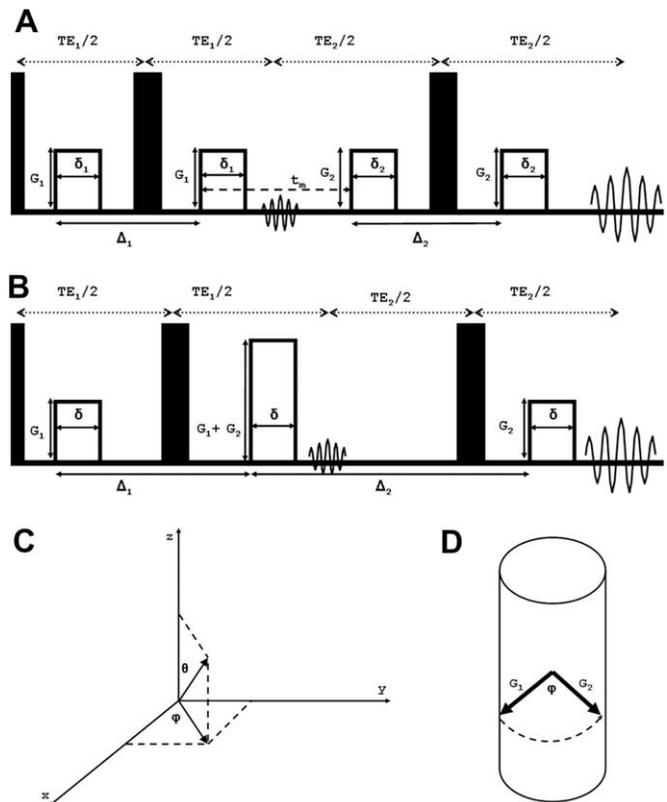

Fig. 1. Sequences and orientation schemes. (A) The d-PGSE experiment in which the mixing time is defined between the beginning of the second diffusion sensitizing gradient and the beginning of the third diffusion sensitizing gradient. (B) The d-PGSE experiment in which the mixing time is inherently 0. The second and the third diffusion sensitizing gradients are superimposed. (C) The azimuthal and polar angles φ and θ, respectively. (D) The orientation of the gradients in one of the angular d-PGSE experiments used in this study, in which the azimuthal angle is varied. In this experiment, $\mathbf{G}_1$ is set along the x-axis, i.e. with $\varphi = 0°$ and $\theta = 90°$, and $\mathbf{G}_2$ is varied along φ in the X–Y plane. Note that the cylinders are aligned with their long axis parallel to the z-axis, which is also the direction of B_0.

measurements. An alternative is to employ extremely strong gradient amplitudes for very short periods; however, such strong gradients also pose a challenge to hardware, and are unlikely to be deemed safe for clinical use because of the large electric fields they can induce. Therefore it remains a challenge to accurately extract the size of small compartments with diffusion MR methods, particularly in a biological or clinical setting.

Mitra studied the angular d-PGSE experiment as early as 1995 [41] in which he predicted the angular dependence of the signal decay from d-PGSE experiments in confined geometries. The theory developed by Mitra did not take into account finite durations of the diffusion sensitizing gradients or the mixing time. However, very recently, Özarslan and Basser addressed the angular dependence of the signal decay in confined geometries theoretically [42] with "arbitrary timing parameters". This study shows, *inter alia*, that when the first gradient is fixed along the axis perpendicular to the fiber, and the direction of the second gradient is varied in the X–Y plane from 0° to 360°, the signal decay exhibits an angular dependence, which can be interpreted as arising from microscopic anisotropy due to the borders of the confining geometry. The theory presented in [42] took into account the duration of the gradient pulses and the mixing time. Moreover, Özarslan and Basser showed that one could circumvent the need for high gradients, and extract the compartment size, even in very small compartments at low q values provided that, $2\pi qa < 1$ for a compartment of size 'a'. Since this method obviates applying very strong gradients for extracting sizes, we have sought to test and

validate these theoretical predictions experimentally. Another recent study which utilized a variant of the d-PGSE and used Mitra's formulation has shown the ability to estimate sizes of restricting compartments, to a certain extent, with relatively low q-values [43]. However, that study was conducted on samples whose dimensions are not exactly known and in which heterogeneity exists. Additionally, sizes were extracted using Mitra's formulation, without accounting for the violation of the SGP approximation or the effect of other experimental parameters.

Therefore, in this study, we aimed at testing the dependence of the signal decay in angular d-PGSE experiments in a well-controlled NMR phantom consisting of water filled microcapillaries with known diameters. We compared the sizes extracted using the theory from both [42] and [41]. To mimic conditions in which diffusion experiments are usually conducted, i.e., that violate the SGP approximation with a range of diffusion timing parameters, we tested the dependence of the signal decay on experimental parameters such as the gradient duration, and the mixing and diffusion times.

2. Materials and methods

All measurements were performed on a Bruker 8.4 T NMR spectrometer capable of producing PFGs up to 190 G/cm in each direction.

Hollow microcapillaries with inner diameters (IDs) of 5 ± 1, 9 ± 1, 10 ± 1 or 19 ± 1 μm (Polymicro Technologies, USA) were immersed in water for several days prior to each experiment. The microcapillaries were packed into a 4 mm glass sleeve which was inserted into a 5 mm NMR tube, aligned with the main axis parallel to the z-direction of the magnet as described previously [21,28,40]. Typical linewidths of 5–15 Hz were obtained after shimming.

Fig. 1 shows the d-PGSE sequences used in this study. Fig. 1A shows a d-PGSE sequence that employs two pairs of diffusion sensitizing gradients, with amplitudes and directions of $\mathbf{G}_1$ and $\mathbf{G}_2$, and gradient durations of δ_1 and δ_2, respectively. The diffusion times Δ_1 and Δ_2 are defined in Fig. 1. In a sequence such as in Fig. 1A, the mixing time, t_m is defined as the time between the end of the Δ_1 period and the beginning of the Δ_2 period. Fig. 1B shows a variant in which the second and third diffusion sensitizing gradients are superimposed, yielding a single pulsed gradient defined by $\mathbf{G}_1 + \mathbf{G}_2$. For this sequence, $t_m = 0$ ms, and in this study we set the durations of the three diffusion sensitizing gradients, δ, to be equal.

Fig. 1C defines the azimuthal angle, φ, and the polar angle, θ. In each experiment, the first gradient pair, $\mathbf{G}_1$, was aligned either along the x-axis or along the z-axis, as shown in Fig. 1C. The orientation of the second gradient pair, $\mathbf{G}_2$, was varied (vide infra). For example, Fig. 1D shows an angular d-PGSE experiment in which $\mathbf{G}_1$ was aligned along the x-axis, and the orientation of $\mathbf{G}_2$ was varied in the X–Y plane. For all of the experiments in this study, the amplitudes of the first and second gradients were identical, i.e., $|\mathbf{G}_1| = |\mathbf{G}_2|$. For all experiments conducted in this study the repetition time (TR) was 3.7 s and the echo times TE_1 and TE_2 (as defined in Fig. 1) were chosen to be as short as possible, and unequal to avoid overlapping echoes. In all experiments performed on microcapillaries in this study, the q-values were chosen to fulfill the requirement $2\pi qa < 1$. However, in some cases, namely when we used 9 ± 1, 10 ± 1 and 19 ± 1 μm microcapillaries, the highest q-value measured, q_{max}, resulted in $2\pi q_{max}a \sim 3$.

The experimental data was rectified to avoid any phase errors.

2.1. Experiments

2.1.1. The angular d-PGSE experiment on an isotropic sample

A 5 mm NMR tube containing a ~1:1 volumetric CH_3OH:D_2O mixture served as an isotropic sample. The sequence shown in Fig. 1B was used. Experiments were conducted with the following parameters: 4 q-values were collected with $\delta = 5$ ms with $G_{max} = 55$ G/cm, resulting in a q_{max} of 1170 cm^{-1}, with $\Delta_1 = \Delta_2 = 15.1$ ms, and the number of scans = 32. In another set of experiments, $\delta = 1.5$ ms with $G_{max} = 55$ G/cm, resulting in $q_{max} = 351$ cm^{-1}, with $\Delta_1 = \Delta_2 = 40$ ms and with the number of scans = 32.

2.2. Varying the polar angle

2.2.1. Varying the polar angle when $\mathbf{G}_1$ is in the z-direction

For this set of experiments, microcapillaries with a nominal ID of 9 ± 1 μm were used. The sequence shown in Fig. 1A was used. For this set of experiments, the direction of $\mathbf{G}_1$ was set with $\varphi = 0°$ and $\theta = 0°$, i.e., along the z-direction. The orientation of $\mathbf{G}_2$ was varied between $\theta = 0°$ (i.e. along the z-axis) and $\theta = 180°$ (i.e., along the z-direction) in 15° intervals, with $\varphi = 0°$ for all experiments (i.e., the axis of symmetry for the rotation of $\mathbf{G}_2$ was the x-axis). For each θ value, 4 q-values were collected with $\delta = 1.5$ ms and $G_{max} = 55$ G/cm, resulting in a $q_{max} = 351$ cm^{-1}, and with $\Delta_1 = \Delta_2 = 40$ ms. The mixing time was set to 5 ms, and the number of scans was set to 128. The results are shown for $q = 129$ cm^{-1} only. One point ($\theta = 75°$) was omitted due to an apparently spurious signal fluctuation.

2.2.2. Varying the polar angle when $\mathbf{G}_1$ is in the x-direction

The same experimental parameters were used, except the direction of $\mathbf{G}_1$ was fixed along the x-axis, i.e., with $\varphi = 0°$ and $\theta = 90°$.

2.3. Varying the azimuthal angle

The rest of the experiments presented in this paper were performed as follows: $\mathbf{G}_1$ was fixed along the x-axis, i.e., with $\varphi = 0°$ and $\theta = 90°$ and the direction of $\mathbf{G}_2$ was varied between $\varphi = 0°$ and $\varphi = 360°$ in 15° increments, with $\theta = 90°$ for all experiments, i.e., in the X–Y plane.

2.3.1. The effect of the compartment size on the signal from the angular d-PGSE experiment

In this set of experiments, 3 separate samples of microcapillaries with nominal IDs of 5 ± 1, 9 ± 1 and 19 ± 1 μm were used. The sequence shown in Fig. 1B was used with the following parameters: For both 5 ± 1 and 9 ± 1 μm ID microcapillaries, 4 q-values were collected with $\delta = 1.5$ ms with $G_{max} = 55$ G/cm resulting in a $q_{max} = 351$ cm^{-1} and with $\Delta_1 = \Delta_2 = 40$ ms. The number of scans = 32. For 19 ± 1 μm microcapillaries 4 points were collected with $\delta = 1.5$ ms and with $G_{max} = 37$ G/cm, resulting in a q_{max} of 236 cm^{-1}, with $\Delta_1 = \Delta_2 = 120$ ms, and with 32 scans.

2.3.2. The effect of prolonging the gradient duration δ

For this set of experiments, microcapillaries with ID = 10 ± 1 μm were used, and the sequence shown in Fig. 1B was employed. Three experiments were conducted in which 4 q-values were collected, and δ was set to 1.5, 4.5 and 7.5 ms with G_{max} of 55, 18.33 and 11 G/cm, respectively, resulting in $q_{max} = 351$ cm^{-1} for all three experiments. The diffusion periods were set to $\Delta_1 = \Delta_2 = 40$ ms and the number of scans was 32.

2.3.3. The effect of prolonging the mixing time

For this set of experiments, microcapillaries with a nominal ID of 10 ± 1 μm were used, with the sequence shown in Fig. 1B for $t_m = 0$ ms and with the sequence shown in Fig. 1A for $t_m > 0$. The following parameters were used: 4 q-values were collected with $\delta = 1.5$ ms with $G_{max} = 55$ G/cm resulting in a $q_{max} = 351$ cm^{-1} and with $\Delta_1 = \Delta_2 = 40$ ms. The number of scans = 32. The mixing time was varied between $t_m = 0$, 5, 20 and 100 ms.

2.3.4. The effect of prolonging the diffusion periods, Δ_1 and Δ_2

For this set of experiments, microcapillaries with ID = 19 ± 1 μm were used, with the sequence shown in Fig. 1B. The following parameters were used: Four q-values were collected with δ = 1.5 ms with G_{max} = 37 G/cm resulting in q_{max} = 236 cm^{-1}. Three experiments were conducted with $\Delta_1 = \Delta_2$ = 7, 30 and 120 ms with number of scans = 32.

2.4. Theory and simulations

As described above, data at several q-values were collected. The theory presented in [42] and [41] provide expressions for the quadratic term of the NMR signal decay. To reduce the effects of higher-order terms in the restricted diffusion experiments, we fitted a function of the form

$$S(q) = S_0 - \alpha q^2 + c q^4$$

to the NMR signal from each direction. In the fitting, a linear least squares estimation algorithm was employed to estimate the quantities, S_0, α, and c. For the NMR signal attenuation, $E(q) = S(q)/S_0$, the above relation can be rewritten as

$$E(q) = 1 - u^2 q^2 + (c/S_0) q^4.$$

Clearly, the quantity $u^2 = \alpha/S_0$ is analogous to a quantity proportional to the mean squared displacement in single-PGSE experiments since it is a measure of the signal decay rate near the origin as can be seen from the expression

$$u^2 = -\frac{d\log E}{dq^2}\bigg|_{q=0}.$$

What is different in double-PGSE acquisitions is that this quantity is a function of the angle between the two gradients (ψ) even when the pore being probed is isotropic (i.e., spherical in 3D and cylindrical in 2D).

In Ref. [42] explicit relationships for the dependence of u^2 on the experimental timing parameters δ, Δ and t_m are provided. Although the theory in Ref. [42] includes generalizations of the problem to different pore shapes, arbitrary tube orientation, orientation distribution functions, etc., here we provide the results relevant to the data collected in this study for brevity.

The NMR signal attenuation can be decomposed into a product of two functions resulting from free and restricted diffusion. The component of the gradient vector along the tube's axis leads to the part of the attenuation due to free diffusion whereas the gradients' component perpendicular to the cylinder's axis will lead to the signal decay due to restricted diffusion.

Note that u^2 determines the signal attenuation value due to restricted diffusion at low q-values. The expressions for the experiments corresponding to the panels a and b of Fig. 1 are given by $u_a^2 = 8\pi^2 r^2 (2A + B\cos\psi)$, and $u_b^2 = 8\pi^2 r^2 (2A + B'\cos\psi)$, respectively, where r is the radius of the cylinders. Here, A, B, and B' are given by the following sums:

$$A = \sum_{n=1}^{\infty} \frac{1}{\beta_n^2(\beta_n^2 - 1)} \left[\frac{2}{\omega_n \delta} - \frac{1}{(\omega_n \delta)^2} \left(2 - 2e^{-\omega_n \delta} \right. \right.$$
$$\left. \left. + e^{-\omega_n(\Delta - \delta)} - 2e^{-\omega_n \Delta} + e^{-\omega_n(\Delta + \delta)} \right) \right]$$

$$B \quad \sum_{n=1}^{\infty} \frac{(\omega_n \delta)^{-2}}{\beta_n^2(\beta_n^2 - 1)} \left(e^{-\omega_n(t_m - \delta)} - 2e^{-\omega_n t_m} \right.$$
$$+ e^{-\omega_n(t_m + \delta)} - 2e^{-\omega_n(\Delta + t_m - \delta)} + 4e^{-\omega_n(\Delta + t_m)}$$
$$- 2e^{-\omega_n(\Delta + t_m + \delta)} + e^{-\omega_n(2\Delta + t_m - \delta)}$$
$$\left. - 2e^{-\omega_n(2\Delta + t_m)} + e^{-\omega_n(2\Delta + t_m + \delta)} \right)$$

$$B' = \sum_{n=1}^{\infty} \frac{1}{\beta_n^2(\beta_n^2 - 1)} \left[\frac{2}{\omega_n \delta} - \frac{1}{\omega_n \delta)^2} \left(2 - 2e^{-\omega_n \delta} \right. \right.$$
$$+ 2e^{-\omega_n(\Delta - \delta)} - 4e^{-\omega_n \Delta} + 2e^{-\omega_n(\Delta + \delta)} - e^{-\omega_n(2\Delta - \delta}$$
$$\left. \left. + 2e^{-2\omega_n \Delta} - e^{-\omega_n(2\Delta + \delta)}) \right]$$

In the above expressions, $\omega_n = \beta_n^2 D/r^2$, where β_n is the nth root of the derivative of the first order Bessel function, i.e., it satisfies the equation $J_1'(\beta_n) = 0$.

The theory in Ref. [41] addresses only the limiting cases of the experimental timing parameters (i.e., $\delta \to 0$, $\Delta \to \infty$ and either $t_m \to 0$ or $t_m \to \infty$). Although no explicit solution for cylindrical pores is provided in Ref. [41], it is straightforward to show that in the simple case of coherently oriented cylinders of radius r, the expected angular dependence in the $\delta \to 0$, $\Delta \to \infty$, and $t_m \to 0$ regime is given by

$$u^2 = \pi^2 r^2 (2 + \cos\psi),$$

where ψ is the angle between the two gradients, both of which are applied perpendicular to the main axis of the cylinder. In this study, the size estimates implied by this function are compared to those obtained using the extended theory in Ref. [42], outlined above.

The NMR signal attenuation due to free diffusion, when the pulse sequence of Fig. 1a is employed, is given by [42]

$$E_a^{\text{free}} = \exp\left(-8\pi^2 q^2 D(\Delta - \delta/3)\right),$$

where D is the free space diffusivity. Similarly, when the pulse sequence of Fig. 1b is used, the NMR signal attenuation resulting from free diffusion is given by [42]

$$E_b^{\text{free}} = \exp\left(-4\pi^2 q^2 D[2(\Delta - \delta/3) - (\delta/3)\cos\psi]\right).$$

In the simulations of echo attenuation from the isotropic methanol sample as well as when the gradient orientation has a component along the main axis of the tubes, the above expressions for free diffusion are employed.

In the estimation of the cylinder radius and the associated standard deviation values, a non-linear curve fitting algorithm that employs Levenberg–Marquardt optimization was used.

3. Results

3.1. Dependence of the angular signal decay from an isotropic sample

In [42], an angular dependence was predicted for the pulse sequence shown in Fig. 1b even for free diffusion, because of the overlap of gradients having finite durations. Fig. 2 shows the results from the angular d-PGSE experiment in which G_1 was fixed along the x-axis and the orientation of G_2 was varied in the X–Y plane, performed on an isotropic sample (methanol in a 5 mm NMR tube). Fig. 2A represents the regime in which the length of the diffusion period is comparable to the diffusion gradient duration ($\Delta_1 = \Delta_2$ = 15.1 ms, δ = 5 ms). As predicted by the theory in [42], an inverted bell-shaped function could be seen for the smaller q values, with a minimum for the polar gradient angle φ = 180°. Fig. 2B shows the regime in which the diffusion periods are relatively long, as compared to the diffusion gradient pulse duration ($\Delta_1 = \Delta_2$ = 40 ms, δ = 1.5 ms), in which the signal exhibits almost no angular variation, as indeed predicted by the theory.

3.2. Varying the polar angle

3.2.1. Varying the polar angle with G_1 set along the x or the z axis

In this experiment, G_1 is fixed along one axis, and the polar angle is varied for G_2. The theory in [42] predicts that the signal decay from such angular d-PGSE experiments should exhibit a bell-
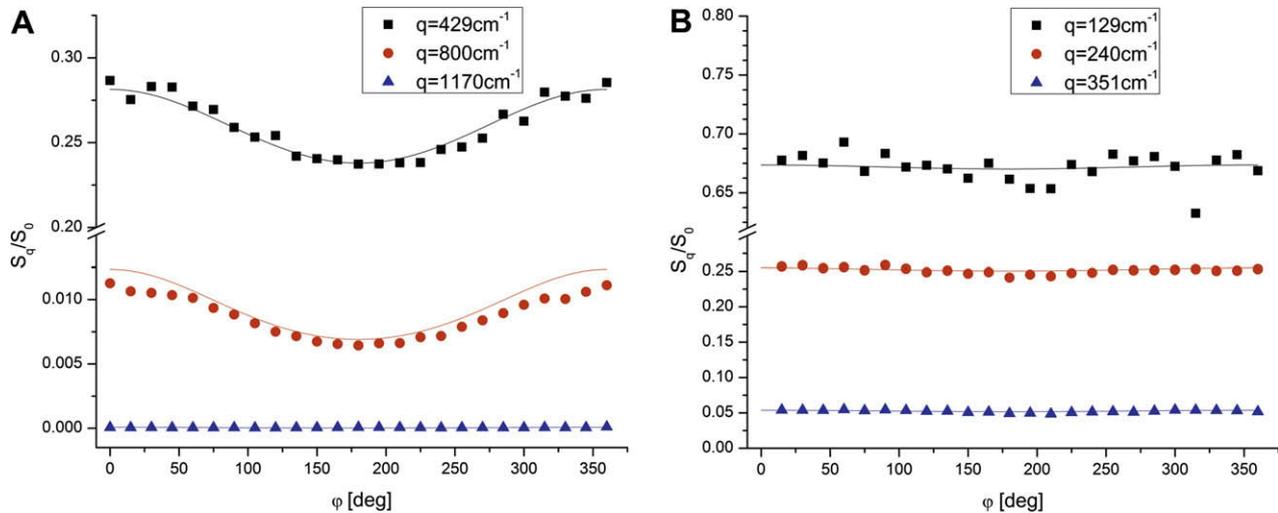
Fig. 2. Angular d-PGSE performed on an isotropic sample with the sequence shown in Fig. 1B. The signal from three different q values is plotted against the azimuthal angle φ. (A) The diffusion periods ($\varDelta_1 = \varDelta_2 = 15.1$ ms) are comparable to the gradient duration ($\delta = 5$ ms). In this case, the theory predicts inverted bell shaped functions. (B) The diffusion periods are long ($\varDelta_1 = \varDelta_2 = 40$ ms) when compared to the gradient duration ($\delta = 1.5$ ms). In this case, only marginal signal variations are expected from the theory. The solid lines represent the simulations.

shaped function with a maximum at 90° when the signal is plotted against the polar angle, θ, and when the microcapillaries are aligned with their main axis parallel to the static magnetic field. Fig. 3 shows the normalized signal obtained from such experiments, performed on microcapillaries with a nominal ID of 9 ± 1 μm, with $q = 129$ cm^{-1}. Two separate experiments are shown: One with $\mathbf{G}_1$ applied along the x-axis (red circles), and one with $\mathbf{G}_1$ applied along the z-axis (black squares). The anticipated bell-shaped functions can be easily seen in Fig. 3. The expected maximum signal indeed occurs at 90° for both experiments, and the simulations fit the experimental points nicely. The signal from the experiment in which $\mathbf{G}_1$ was applied along the z-axis exhibited a 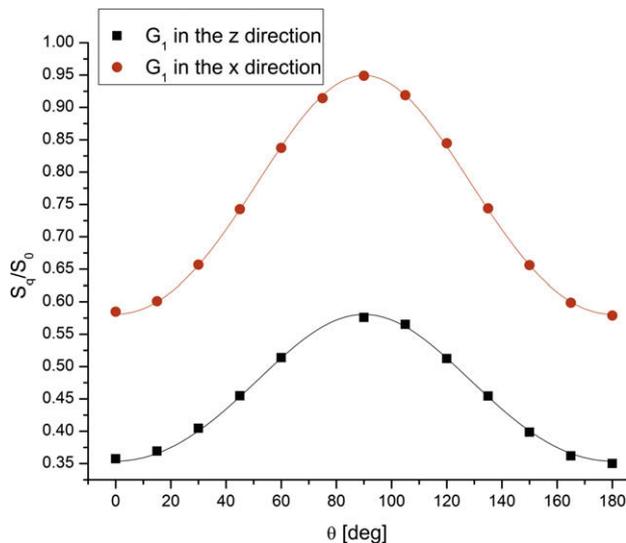stronger attenuation of the signal when compared to the experiment in which $\mathbf{G}_1$ was applied along the x-axis. The percent signal difference that was measured between $\theta = 0°$ and $\theta = 90°$ for both experiments was $\sim 38\%$ of the maximum signal. The IDs that were extracted were 8.39 ± 0.47 and 8.30 ± 0.07 μm for the experiments in which $\mathbf{G}_1$ was applied in the z- and x-axes, respectively, which are in good agreement with the 9 ± 1 μm nominal ID of the microcapillaries used.

3.3. Varying the azimuthal angle

All of the following experiments in this study were conducted with $\mathbf{G}_1$ along the x-axis, and the azimuthal angle, φ, of $\mathbf{G}_2$ was varied with $\theta = 90°$ (i.e., in the X–Y plane). The expected bell-shaped functions occur for each individual q-value (data not shown) obtained in our measurements, however, we decided to combine the 4 q-values and plot the attenuation factor u^2 versus φ (see Section 2). The theory in [42] predicts an inverted bell-shaped function for this kind of plot.

3.3.1. Dependence of the signal decay on the size of the compartment
Fig. 4 shows the attenuation factor, u^2, as a function of φ, for three different samples of microcapillaries having nominal IDs of 5 ± 1, 9 ± 1 and 19 ± 1 μm. The expected inverted bell-shaped functions can be seen for all experiments. The sizes, extracted from the fit of the angular dependence, closely correspond to the nominal ID and are summarized in Table 1. Note, that when extracting the signal in the limiting cases of Ref. [41], the finiteness of the durations and separations of the gradients are not accounted for. Therefore a smaller size is extracted for the 5 ± 1 and 9 ± 1 μm microcapillaries. The violation of the SGP approximation is not as important for the 19 ± 1 μm microcapillaries, therefore both analyses resulted in similar extracted sizes.

3.3.2. Dependence of the angular signal decay on the gradient duration
To test the effect of violating the SGP approximation, we used 10 ± 1 μm ID microcapillaries and gradually prolonged δ_1 and δ_2. Fig. 5A shows the dependence of the angular signal decay on the duration of the gradients. The attenuation factor u^2 values decrease with increasing δ, because of the gradual violation of the SGP approximation. Note that in this set of experiments the amplitude of the gradients was calculated such that the same q values were
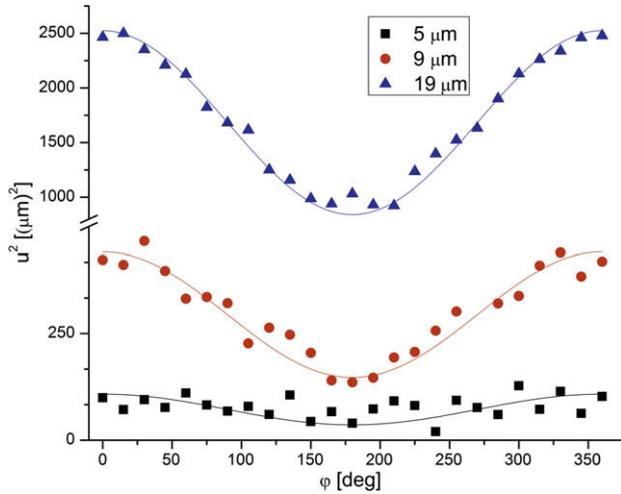

Fig. 3. Variation of the polar angle θ. This set of experiments was performed with the sequence shown in Fig. 1A on microcapillaries with a nominal ID of 9 ± 1 μm. The angular signal dependence is shown for experiments in which $\mathbf{G}_1$ was applied in the z (black square) or x (red circles) directions, and the polar angle of $\mathbf{G}_2$ was varied. The bell shaped function can be easily seen. The solid lines represent the simulations for these experiments. One point in one of the experiments was omitted due to a signal fluctuation. (For interpretation of color mentioned in this figure the reader is referred to the web version of the article.)

Fig. 4. Effect of the compartment size on the angular signal variation. The angular d-PGSE experiment in which the azimuthal angle φ is varied when $\mathbf{G}_1$ is fixed along the x-axis performed with the sequence shown in figure 1B on microcapillaries with a nominal ID of 5 ± 1, 9 ± 1 and 19 ± 1 μm. The solid lines represent the simulations for these experiments. For all of these experiments, the diffusion periods were long enough to probe the boundaries of the restricting geometry.

Table 1

Summary of the sizes extracted using the theory in reference [42] (left column) and the limiting case in reference [41] (right column). The results from top to bottom indicate the different experiments shown in this study: the variation of size, prolongation of the gradient duration, prolongation of the mixing time and variation in the diffusion periods.

	ID (μm) estimations based on Ref. [42]	ID (μm) estimations based on Ref. [41]
Variable ID		
ID = 5 ± 1 μm	4.91 ± 0.12	3.82 ± 0.14
ID = 9 ± 1 μm	8.48 ± 0.07	7.72 ± 0.08
ID = 19 ± 1 μm	18.85 ± 0.08	18.46 ± 0.08
Nominal ID = 10 ± 1 μm		
δ = 1.5 ms	10.22 ± 0.05	9.56 ± 0.05
δ = 4.5 ms	10.34 ± 0.06	8.66 ± 0.06
δ = 7.5 ms	10.46 ± 0.09	7.97 ± 0.10
Nominal ID = 10 ± 1 μm		
t_m = 0 ms	10.37 ± 0.03	9.72 ± 0.04
t_m = 5 ms	10.33 ± 0.05	9.24 ± 0.23
t_m = 20 ms	10.32 ± 0.04	9.04 ± 0.32
t_m = 100 ms	10.37 ± 0.04	9.06 ± 0.34
Nominal ID = 19 ± 1 μm		
Δ = 7 ms	27.77 ± 1.85	12.08 ± 0.31
Δ = 30 ms	19.08 ± 0.09	17.49 ± 0.11
Δ = 100 ms	18.85 ± 0.08	18.46 ± 0.08

obtained for all δ values. For δs of 1.5, 4.5 and 7.5 ms, the extracted IDs were 10.22 ± 0.05, 10.34 ± 0.06 and 10.46 ± 0.09 μm, respectively, (Table 1), indicating that the gradient pulse duration was indeed accounted for. The IDs that were extracted in the regime considered by Mitra showed a reduction in the compartment size, as expected from the violation of the SGP approximation.

3.3.3. Dependence of the signal decay on the mixing time (t_m)

Fig. 5B shows the plot of the attenuation factor, u^2, versus the azimuthal angle, φ, with different mixing times. When $t_m = 0$ ms, a clear inverted bell-shaped function can be seen. Successive prolongation of the mixing time to 5, 20 and 100 ms resulted in a gradual loss of the inverted bell-shape. For $t_m = 0$, 5, 20 and 100 ms the extracted IDs were 10.37 ± 0.03, 10.33 ± 0.04, 10.32 ± 0.03 and
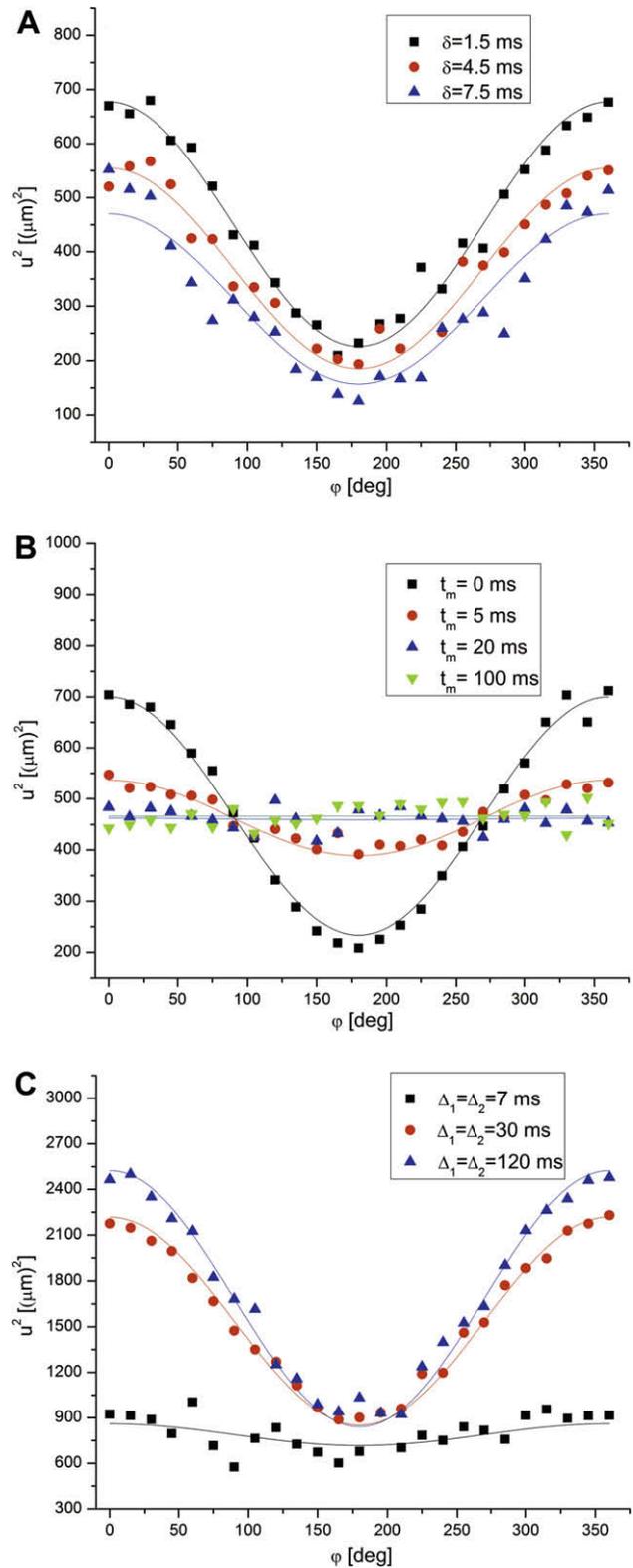

Fig. 5. The effect of experimental parameters on the angular signal variation. (A) The effect of prolonging the gradient durations δ_1 and δ_2. (B) The effect of prolonging the mixing time (t_m). Both (A) and (B) were performed on microcapillaries with a nominal ID of 10 ± 1 μm, with diffusion periods $\Delta_1 = \Delta_2 = 40$ ms, long enough to probe the boundaries of the restricting compartment. (C) The effect of concomitantly prolonging the diffusion periods Δ_1 and Δ_2, performed on microcapillaries with a nominal ID of 19 ± 1 μm with $\delta_1 = \delta_2 = 1.5$ ms, not long enough to significantly violate the SGP approximation. The solid lines in A–C represent the simulations for these experiments.

10.37 ± 0.04 μm, respectively, (Table 1). The extracted sizes correspond very well to the nominal ID of 10 ± 1 μm, even for very long mixing times. Note that these values are also in agreement with those obtained by prolonging δ.

On the other hand, the IDs extracted using Mitra's formulae decrease significantly as mixing time is increased. As expected, the best agreement was achieved at t_m = 0. However, the sizes that were extracted were consistently smaller, even at t_m = 0, probably because this method does not account for the finite duration of the gradients (Table 1).

3.3.4. Dependence of the signal decay on the diffusion periods

In this set of experiments, the diffusion periods Δ_1 and Δ_2 were concomitantly prolonged from 7 ms (i.e., not long enough to probe the boundaries of the 19 ± 1 μm microcapillaries) to 30 and 100 ms. Fig. 5C shows that little angular dependence was observed for the short diffusion times, while the simulations produced an inaccurate estimate of the ID = 27.77 ± 1.85 μm. However, prolonging the diffusion period resulted in the expected inverted bell-shaped functions, and accurate estimates of compartment size from the simulations (Fig. 5C and Table 1). For the longest diffusion period, Mitra's formulation extracted an accurate size, probably because the SGP violation is much less important for compartments with larger radii (in this case, 19 ± 1 μm microcapillaries).

4. Discussion

Obtaining structural information from ordered arrays or packs is important in a variety of problems related to porous materials and biological tissues [8,13]. As diffusion NMR methods are non-invasive, they provide one of the most convenient means for extracting the dimensions of the compartments of interest [10]. The s-PGSE experiment has been able to accurately extract pore dimensions from a wide range of ordered samples, especially when utilizing the diffusion–diffraction phenomenon [21,22,24–26,30]. The diffusion–diffraction patterns can accurately represent the size and shape of the compartment, provided that the SGP approximation is not violated. However, even the first diffraction trough becomes elusive in very small compartments, as the SGP approximation is rapidly violated and the diffraction is shifted towards a higher, sometimes unattainable q value. This underscores the need for methods that provide the same structural information at lower q values, enabling the use of low-amplitude pulsed gradients.

In this study, we have shown that the angular d-PGSE experiment may be used to accurately obtain the same structural information that can be obtained from high-q measurements. The angular d-PGSE experiment appears to circumvent the need for strong gradients, as the basic constraint is that $2\pi qa \leqslant 1$ (where 'a' is the compartment dimension). For example, the diffraction from 5 μm ID microcapillaries is expected at q = 2440 cm^{-1}. However, to reach this q-value with our gradient system capable of producing 190 G/cm in all three directions, a δ of at least 3.5 ms needs to be employed, significantly violating the SGP approximation and shifting the diffraction towards even higher q-values. Therefore, with our hardware, diffractions are not observable for 5 μm microcapillaries (data not shown). However, using the angular d-PGSE experiment we could easily extract the accurate size. Interestingly, when we used Mitra's limiting values for the experimental parameters to extract the compartment dimension, a smaller size was obtained, which is a result of violating the narrow pulse condition. Note that the deviation from the correct values will be even more significant in smaller compartments when the timing parameters are not taken into consideration. This is also manifested in the larger standard deviations that were observed when sizes were extracted using Mitra's formulation with varying mixing times.

In small compartments, one of the problems in extracting the accurate compartment size is that the SGP approximation is easily violated, even when the gradient duration is short. In this study, we have shown that by using the formulations in [42], we could correct for violation of the SGP approximation. Even when we set δ to 7.5 ms, which significantly violates the SGP approximation in 10 μm ID microcapillaries, we could extract the accurate diameter of the microcapillaries.

In this study, we have validated the anticipated bell-shaped functions for angular d-PGSE experiments in which the polar angle was varied. The maximum occurs when the second gradient is applied perpendicular to the main axis of the microcapillaries. The signal attenuation in the experiment in which G_1 was set in the z-direction was stronger when compared to the experiment in which G_1 was set in the x-direction. This can be explained by the stronger diffusion weighting experienced by the spins undergoing free diffusion during the first encoding period in the z-direction. Note that this type of angular d-PGSE experiment may be used to reveal the orientation of the fibers. However, since a significant portion of the signal attenuation is due to free diffusion in these experiments, accurate estimation of the capillary size necessitates *a-priori* knowledge of the bulk diffusivity. When both gradients are applied perpendicular to the main axis of the microcapillaries, the sensitivity of the estimated parameters to the errors in bulk diffusivity is significantly reduced, suggesting that these kind of experiments are more suitable for extraction of compartment sizes.

In this study, we also performed the angular d-PGSE experiment with different mixing times. Prolonging the mixing time reduces the correlation between the two pairs of diffusion gradient encodings [39,40]. Therefore, the anisotropy induced by the boundaries is diminished as t_m is prolonged. This is manifested in a gradual loss of the curvature in the bell-shaped functions. However, the simulations could still accurately extract the pore dimension, even at long mixing times.

When we tested the effect of shortening the diffusion periods Δ_1 and Δ_2 we found that, as predicted [42], they have to be long enough to probe the boundaries of the confining compartment, i.e., for pore of dimension 'a', this occurs when $\Delta = a^2/2D$. When the diffusion periods are not long enough, simulations could not extract an accurate size as can be seen from the $\Delta_1 = \Delta_2 = 7$ ms experiments on 19 μm ID tubes, i.e., when $D\Delta/a^2 = 0.155$. The deviation from the expected ID does not suggest an error in the theory. Rather, the percentage of the spins that feel the boundaries are so small in such large tubes that restricted diffusion is not achieved. In fact, for this combination of diffusion time and ID, the u^2 value that would be observed from purely free diffusion is $\sim$1000 μm^2—only slightly above the experimentally observed values. In addition, note that in small pores, the requirement of $\Delta = a^2/2D$ can be satisfied with rather short diffusion periods. For example, in neuronal tissue, the axon may have diameters as small as 1–2 μm, so a diffusion period of $\sim$5 ms would suffice for water to completely probe their boundaries. This was recently shown to be the case in q-space single PGSE experiments performed on nerves, in which the diffusion time was varied in small intervals from very short to long diffusion times (i.e., Δ was varied from 3.7 to 99.3 ms) [17].

From our measurements, the optimal conditions of the angular d-PGSE experiments are highlighted. Without correcting for violation of the SGP approximation, an angular d-PGSE experiment employing short gradient durations with low amplitude gradients (such that $2\pi qa \sim 1$), with t_m = 0 ms and diffusion periods that are sufficiently long to probe the borders of the confining geometry will result in a pronounced bell-shaped function, from which the size of the compartment can be extracted. Note that the sequence shown in Fig. 1B is advantageous in that t_m = 0 ms, however, it requires a stronger gradient system, as the middle gradient is a

superposition of $\mathbf{G}_1$ and $\mathbf{G}_2$. This is not the case for the sequence shown in Fig. 1A; the gradients are not superimposed. However, in the sequence shown in Fig. 1A, the mixing time cannot be effectively set to zero, and must equal to at least δ_1. In pores of very small dimensions, this may pose a problem. However, when analyzing the results with the theory shown in [42], arbitrary timing parameters can be used to extract the size accurately, provided that the diffusion periods are sufficiently long to probe the boundaries. The experiment in which $\mathbf{G}_1$ is fixed along the x-axis and the orientation of $\mathbf{G}_2$ is varied in the X–Y plane seems to have several advantages: The sensitivity to microscopic anisotropy is larger as both of the diffusion sensitizing gradient pairs are in the plane perpendicular to the main axis of the fiber, the size estimates are weakly dependent on the diffusion coefficient, and the SNR is higher because both gradient pairs encode restricted diffusion so less signal is lost to dephasing.

In theory, if the pore shape is known *a priori*, one can extract the size of the compartment even from low q s-PGSE experiments. However, in this case, the observed signal attenuation will not reveal whether the diffusion regime is truly restricted—only the diffraction minima, at high q-values provide the actual signature for restricted diffusion. The advantage of d-PGSE is that it provides a conclusive signature that arises from microscopic anisotropy (angular dependence of the signal decay) for restriction at very low q-values. Another point is that the best estimate for size is obtained when parameters are varied over a wide range. In s-PGSE, this means going to higher q-values. In the low-q angular d-PGSE, q is fixed and the large range of parameters is achieved by varying the angles between $0°$ and $360°$.

Note that in all the phantoms we employed, the tubes were aligned with the main magnetic field (z-axis). Therefore, it was possible to measure the diameter of the tubes simply by applying the gradients in the transverse plane. Importantly, when the orientation is not known *a priori*, it can be measured using a more general sampling scheme and Eqs. (14–16) in Ref. [42], which would yield the orientations as well as the diameters of the cylinders simultaneously. Moreover, the subsequent formulation based on the relations validated in this study makes it possible to obtain even an orientation distribution function for tubes from the quadratic term of the NMR signal attenuation. Measuring the pore size, orientation and distribution may have applications in biological tissues, porous media, and emulsions, all of which exhibit different levels of diffusion complexity; further studies are needed to demonstrate the full capabilities of d-PGSE in characterizing these systems.

One potential limitation of the angular d-PGSE experiment is that low gradients may be unstable (especially in systems capable of producing very strong pulsed gradients) producing fluctuating MR signals even though the SNR is high. For clinical systems, however, this should not pose a serious problem.

Although many angles are required to achieve high angular resolution, these can be collected in a rather short time because the minimum measurement involves acquisition of only two q-values. Since the SNR is high due to the low q-values used, relatively few averages are needed. Therefore, a high angular resolution can be achieved in a time-efficient manner.

Our findings imply that for relatively small pores, in which very high q-values are needed to characterize the pore dimension, the low-q regime angular d-PGSE experiment may provide an alternative to estimating the pore dimension. We observed that in small pores, the SGP approximation is easily violated and the diffusion period easily probes the boundaries of the restricting compartment. As we have shown in this study, under these conditions, the simulations can accurately characterize the compartment size if the experimental timing parameters are taken into account. Since the theory correctly accounts for the timing parameters, more general acquisition strategies that involve angular variations

as well as variations in the timing parameters can be devised. Such acquisitions, with increased dimensionality of sampled parameter space, may help elucidate more features related to the microstructure of the specimen. These findings are important in studying small and complicated pore structures such as those found in biological tissue.

5. Conclusions

We have demonstrated the feasibility of employing low amplitude gradients to estimate the pore dimensions in restricted compartments. We can accurately estimate pore dimensions when the timing parameters of the double-PGSE experiments are incorporated into our simulations, provided that the diffusion times are long enough to enable diffusing molecules to probe the boundaries of the confining compartment. This experimental study validates the theory that was previously published [41,42]. We conclude that for restricted diffusion in confined geometries characterized by small dimensions, the low q angular d-PGSE experiment may be more advantageous than the s-PGSE experiment for extracting structural information, as it employs low amplitude gradients and inherently has a higher SNR.

Acknowledgments

References

[1] E.O. Stejskal, J.E. Tanner, Spin diffusion measurements—spin echoes in presence of a time-dependent field gradient, J. Chem. Phys. 42 (1965) 288–292.

[2] P. Stilbs, Fourier transform pulsed-gradient spin-echo studies of molecular diffusion, Prog. Nuclear Magn. Reson. Spectrosc. 19 (1987) 1–45.

[3] Y. Cohen, L. Avram, L. Frish, Diffusion NMR spectroscopy in supramolecular and combinatorial chemistry: an old parameter—New insights, Angew. Chem. Int. Ed. 44 (2005) 520–554.

[4] M. Stjerndahl, D. Lundberg, H.L. Zhang, F.M. Menger, NMR studies of aggregation and hydration of surfactants containing amide bonds, J. Phys. Chem. B 111 (2007) 2008–2014.

[5] P.S. Pregosin, P.G.A. Kumar, I. Fernandez, Pulsed gradient spin-echo (PGSE) diffusion and H-1, F-19 heteronuclear overhauser spectroscopy (HOESY) NMR methods in inorganic and organometallic chemistry: something old and something new, Chem. Rev. 105 (2005) 2977–2998.

[6] L.H. Lucas, C.K. Larive, Measuring ligand–protein binding using NMR diffusion experiments, Concepts Magn. Reson. A 20A (2004) 24–41.

[7] W.S. Price, Pulsed-field gradient nuclear magnetic resonance as a tool for studying translational diffusion 1, Basic Theory, Concepts Magn. Reson. 9 (1997) 299–336.

[8] P.T. Callaghan, NMR imaging, NMR diffraction and applications of pulsed gradient spin echoes in porous media, Magn. Reson. Imaging 14 (1996) 701–709.

[9] P.W. Kuchel, A. Coy, P. Stilbs, NMR "diffusion–diffraction" of water revealing alignment of erythrocytes in a magnetic field and their dimensions and membrane transport characteristics, Magn. Reson. Med. 37 (1997) 637–643.

[10] Y. Cohen, Y. Assaf, High b-value q-space analyzed diffusion-weighted MRS and MRI in neuronal tissues—a technical review, NMR Biomed. 15 (2002) 516–542.

[11] P.J. Basser, J. Mattiello, D. Lebihan, Estimation of the effective self-diffusion tensor from the NMR spin-echo, J. Magn. Reson. B 103 (1994) 247–254.

[12] T. Niendorf, R.M. Dijkhuizen, D.G. Norris, M.V. Campagne, K. Nicolay, Biexponential diffusion attenuation in various states of brain tissue: implications for diffusion-weighted imaging, Magn. Reson. Med. 36 (1996) 847–857.

[13] Y. Assaf, Y. Cohen, Non-mono-exponential attenuation of water and N-acetyl aspartate signals due to diffusion in brain tissue, J. Magn. Reson. 131 (1998) 69–85.

[14] R.V. Mulkern, H. Gudbjartsson, C.F. Westin, H.P. Zengingonul, W. Gartner, C.R.G. Guttmann, R.L. Robertson, W. Kyriakos, R. Schwartz, D. Holtzman, F.A. Jolesz, S.E. Maier, Multi-component apparent diffusion coefficients in human brain, NMR Biomed. 12 (1999) 51–62.

[15] Y. Assaf, D. Ben-Bashat, J. Chapman, S. Peled, I.E. Biton, M. Kafri, Y. Segev, T. Hendler, A.D. Korczyn, M. Graif, Y. Cohen, High b-value q-space analyzed diffusion-weighted MRI: application to multiple sclerosis, Magn. Reson. Med. 47 (2002) 115–126.

[16] P.W. Kuchel, T.R. Eykyn, D.G. Regan, Measurement of compartment size in q-space experiments: Fourier transform of the second derivative, Magn. Reson. Med. 52 (2004) 907–912.

[17] A. Bar-Shir, Y. Cohen, High b-value q-space diffusion MRS of nerves: structural information and comparison with histological evidence, NMR Biomed. 21 (2008) 165–174.

[18] H.H. Ong, A.C. Wright, S.L. Wehrli, A. Souza, E.D. Schwartz, S.N. Hwang, F.W. Wehrli, Indirect measurement of regional axon diameter in excised mouse spinal cord with q-space imaging: simulation and experimental studies, Neuroimage 40 (2008) 1619–1632.

[19] P.T. Callaghan, A. Coy, D. Macgowan, K.J. Packer, F.O. Zelaya, Diffraction-like effects in NMR diffusion studies of fluids in porous solids, Nature 351 (1991) 467–469.

[20] D.G. Cory, A.N. Garroway, Measurement of translational displacement probabilities by NMR—an indicator of compartmentation, Magn. Reson. Med. 14 (1990) 435–444.

[21] L. Avram, Y. Assaf, Y. Cohen, The effect of rotational angle and experimental parameters on the diffraction patterns and micro-structural information obtained from q-space diffusion NMR: implication for diffusion in white matter fibers, J. Magn. Reson. 169 (2004) 30–38.

[22] L. Avram, E. Özarslan, Y. Assaf, A. Bar-Shir, Y. Cohen, P.J. Basser, Three-dimensional water diffusion in impermeable cylindrical tubes: theory versus experiments, NMR Biomed. 21 (2008) 888–898.

[23] A.V. Barzykin, Theory of spin echo in restricted geometries under a step-wise gradient pulse sequence, J. Magn. Reson. 139 (1999) 342–353.

[24] P.T. Callaghan, Pulsed-gradient spin-echo NMR for planar, cylindrical, and spherical pores under conditions of wall relaxation, J. Magn. Reson. A 113 (1995) 53–59.

[25] S.L. Codd, P.T. Callaghan, Spin echo analysis of restricted diffusion under generalized gradient waveforms: planar, cylindrical, and spherical pores with wall relaxivity, J. Magn. Reson. 137 (1999) 358–372.

[26] B.N. Ryland, P.T. Callaghan, Spin echo analysis of restricted diffusion under generalized gradient waveforms for spherical pores with relaxivity and interconnections, Isr. J. Chem. 43 (2003) 1–7.

[27] A. Bar-Shir, Y. Cohen, The effect of the rotational angle on MR diffusion indices in nerves: is the rms displacement of the slow-diffusing component a good measure of fiber orientation?, J Magn. Reson. 190 (2008) 33–42.

[28] A. Bar-Shir, L. Avram, E. Özarslan, P.J. Basser, Y. Cohen, The effect of the diffusion time and pulse gradient duration ratio on the diffraction pattern and the structural information estimated from q-space diffusion MR: experiments and simulations, J. Magn Reson. 194 (2008) 230–236.

[29] D.G. Cory, A.N. Garroway, J.B. Miller, Applications of spin transport as a probe of local geometry, Polym. Preprints 31 (1990) 149.

[30] P.T. Callaghan, S.L. Codd, J.D. Seymour, Spatial coherence phenomena arising from translational spin motion in gradient spin echo experiments, Concepts Magn. Reson. 11 (1999) 181–202.

[31] P.T. Callaghan, S. Godefroy, B.N. Ryland, Use of the second dimension in PGSE NMR studies of porous media, Magn. Reson. Imaging 21 (2003) 243–248.

[32] P. Galvosas, Y. Qiao, M. Schonhoff, P.T. Callaghan, On the use of 2D correlation and exchange NMR spectroscopy in organic porous materials, Magn. Reson. Imaging 25 (2007) 497–500.

[33] A. Jerschow, N. Muller, Suppression of convection artifacts in stimulated-echo diffusion experiments. Double-stimulated-echo experiments, J. Magn. Reson. 125 (1997) 372–375.

[34] P.T. Callaghan, A.A. Khrapitchev, Time-dependent velocities in porous media dispersive flow, Magn. Reson. Imaging 19 (2001) 301–305.

[35] A.A. Khrapitchev, S. Stapf, P.T. Callaghan, NMR visualization of displacement correlations for flow in porous media, Phys. Rev. E 66 (2002).

[36] P.T. Callaghan, M.E. Komlosh, Locally anisotropic motion in a macroscopically isotropic system: displacement correlations measured using double pulsed gradient spin-echo NMR, Magn. Reson. Chem. 40 (2002) S15–S19.

[37] M.E. Komlosh, F. Horkay, R.Z. Freldlin, U. Nevo, Y. Assaf, P.J. Basser, Detection of microscopic anisotropy in gray matter and in a novel tissue phantom using double-pulsed gradient spin echo MR, J. Magn. Reson. 189 (2007) 38–45.

[38] M.E. Komlosh, M.J. Lizak, F. Horkay, R.Z. Freidlin, P.J. Basser, Observation of microscopic diffusion anisotropy in the spinal cord using double-pulsed gradient spin echo MRI, Magn. Reson. Med. 59 (2008) 803–809.

[39] E. Özarslan, P.J. Basser, MR diffusion–"diffraction" phenomenon in multi-pulse-field-gradient experiments, J. Magn. Reson. 188 (2007) 285–294.

[40] N. Shemesh, Y. Cohen, The effect of experimental parameters on the signal decay in double-PGSE experiments: negative diffractions and enhancement of structural information, J. Magn. Reson. 195 (2008) 153–161.

[41] P.P. Mitra, Multiple wave–vector extensions of the NMR pulsed-field-gradient spin-echo diffusion measurement, Phys. Rev. B 51 (1995) 15074–15078.

[42] E. Özarslan, P.J. Basser, Microscopic anisotropy revealed by NMR double pulsed field gradient experiments with arbitrary timing parameters, J. Chem. Phys. 128 (2008) 154511.

[43] M.A. Koch, J. Finsterbusch, Compartment size estimation with double wave vector diffusion-weighted imaging, Magn. Reson. Med. 60 (2008) 90–101.